SCIENTIFIC REPORTS

OPEN

Rational design of inorganic dielectric materials with expected permittivity

Received: 28 June 2015
Accepted: 20 October 2015
Published: 30 November 2015

Congwei Xie[1,2], Artem R. Oganov[1,3,4,5], Dong Dong[1,2], Ning Liu[1,2], Duan Li[1,2] & Tekalign Terfa Debela[1,2]

Techniques for rapid design of dielectric materials with appropriate permittivity for many important technological applications are urgently needed. It is found that functional structure blocks (FSBs) are helpful in rational design of inorganic dielectrics with expected permittivity. To achieve this, coordination polyhedra are parameterized as FSBs and a simple empirical model to evaluate permittivity based on these FSB parameters is proposed. Using this model, a wide range of examples including ferroelectric, high/low permittivity materials are discussed, resulting in several candidate materials for experimental follow-up.

Dielectric materials are essential for many technological applications in optical, electronic, and micro-electronic devices. For instance, high-permittivity materials are required for gate dielectrics and high-energy storage capacitors, and low-permittivity dielectrics are necessary for transparent windows and miniaturized integrated circuits. The search for these dielectric materials over a wide range of compounds is time-consuming. A major reason is the lack of a clear and intuitive data set to give an idea about which materials should be focused on[1]. Fortunately, we now have computational tools such as codes based on density functional theory[2,3] (DFT), capable of accurately predicting many important materials properties. With the help of computations, materials discovery can be accelerated[4–6].

Up to now, high-throughput computational approach have been employed to screen thousands of compounds for new materials[7–14]. Structure prediction methods[15], such as USPEX[16,17], have also been developed to optimize certain properties of materials with only the chemical composition given[18–21]. However, the efficiency of these theoretical methods requires a fast and accurate evaluation of the properties of interest, while dielectric properties are relatively time-consuming. Therefore, it would be desirable to find a way to compute them from crystal structure, most transparently using functional structure blocks (FSBs), which are directly linked to the materials properties. The application of this FSB method mainly depends on: (1) the determination of a suitable FSB for a certain property of materials; and (2) the establishment of an explicit relationship between this property and its FSB. With such structure-property relations, one can quantitatively or qualitatively evaluate properties for a material in seconds. In this paper, we will demonstrate that the idea of FSBs could be very useful for rational design of materials with expected permittivity.

Inspired by Rignanese *et al.*[22] and our previous studies[21,23], we choose the coordination polyhedron as FSB for permittivity due to its major and easy to rationalize effect on permittivities of materials. Coordination polyhedron to a very large extent determines many aspects of lattice dynamics and thus

[1]International Center for Materials Discovery, School of Materials Science and Engineering, Northwestern Polytechnical University, Xi'an, Shaanxi 710072, P.R. China. [2]Science and Technology on Thermostructural Composite Materials Laboratory, School of Materials Science and Engineering, Northwestern Polytechnical University, Xi'an, Shaanxi 710072, P.R. China. [3]Skolkovo Institute of Science and Technology, 3 Nobel St., Skolkovo 143025, Russia. [4]Moscow Institute of Physics and Technology, 9 Institutskiy Lane, Dolgoprudny City, Moscow Region 141700, Russia. [5]Department of Geosciences and Center for Materials by Design, Stony Brook University, Stony Brook, New York 11794, USA. Correspondence and requests for materials should be addressed to C.X. (email: xiecw1021@mail.nwpu.edu.cn) or A.R.O. (email: artem.oganov@stonybrook.edu)

can be used to determine permittivity[21,22]. Rignanese *et al.*[22] proposed an empirical model to calculate permittivity, for each coordination polyhedron using three characteristic parameters (electronic polarizability α, charge Z, and force constant C). In this present study, we suggest a simplified empirical model with each type of coordination polyhedra characterized by two parameters: electronic polarizability α and ionic oscillator strength η. Furthermore, by introducing the volume V of each type of polyhedron, we can extend our model to estimate permittivity of a crystal structure provided that the type of coordination polyhedron is known. This means that dielectric materials with expected permittivity could be constructed by selecting appropriate coordination polyhedra.

Results and Discussions

Description of the model. According to Rignanese's model[22], it is possible to evaluate the electronic[24], lattice, and static permittivities of a given structure based on its electronic polarizability α, charge Z, and force constant C:

$$\frac{\varepsilon_\infty - 1}{\varepsilon_\infty + 2} = \frac{4\pi}{3V}\alpha, \tag{1}$$

$$\varepsilon_L = \varepsilon_0 - \varepsilon_\infty = \frac{4\pi}{V}\frac{Z^2}{C}, \tag{2}$$

where ε_∞ is the electronic permittivity; ε_L is the lattice permittivity; ε_0 is the static permittivity; and V is the volume of the structure. They define α_i, Z_i, and C_i values for each type of coordination polyhedron i, and assuming that:

$$\alpha = \sum_i n_i\alpha_i\ , \quad Z^2 = \sum_i n_i {Z_i}^2 \text{ and } C^{-1} = \sum_i n_i {C_i}^{-1}, \tag{3}$$

where n_i is the number of type-i coordination polyhedron contained in a structure. Summation is done over all types of coordination polyhedra. The optimal α_i, Z_i, and C_i values for each type of coordination polyhedron i can be determined using least-squares method based on the ε_∞, ε_L, and ε_0 values calculated from first principles for a set of materials. However, ε_L obtained by their model is sometimes very different from that calculated from first principles. This may be due to the fact that Z and C are considered as two independent variables in their model, which, however, may be correlated to each other. Therefore, we suggest defining a single parameter of ionic oscillator strength η:

$$\eta = \frac{Z^2}{C}. \tag{4}$$

Then, the lattice permittivity ε_L can be calculated as:

$$\varepsilon_L = \varepsilon_0 - \varepsilon_\infty = \frac{4\pi}{V}\eta. \tag{5}$$

By analogy with α_i, we define η_i for each type of coordination polyhedron i such that:

$$\eta = \sum_i n_i\eta_i. \tag{6}$$

The optimal values η_i can be determined in the same way as for α_i. As shown in the following part of this paper, ε_L obtained from our simplified model improve upon those calculated from Rignanese's model in most cases.

Test of the model. We have calculated permittivity of various inorganic compounds constructed from three binary oxide systems (MgO, Al_2O_3, and SiO_2). With the crystal structures of these compounds obtained from Materials Project[1], we performed full structure relaxation before calculating permittivity using the density functional perturbation theory (DFPT[25]) approach. Structural information and DFPT permittivities of these compounds can be found as Supplementary Table Is. The optimal α and η values of seven coordination polyhedra, MgO_4, MgO_6, AlO_4, AlO_5, AlO_6, SiO_4, and SiO_6 obtained in our model are listed in Table 1.

In Fig. 1, α and η values of MgO, Al_2O_3, and SiO_2 compounds given by our model are compared to those calculated from DFPT approach, with quite good agreement for most of the structures. In particular, α values obtained in our model agree very well with those computed by the DFPT approach, with an average relative error as low as 1.5%. Although a few η values have error higher than 10%, it can be

Coordination polyhedron	α	η	V	α/V	η/V
LiO_4	1.16	4.79	12.42	0.093	0.386
LiF_6	1.03	11.54	16.75	0.061	0.689
BeO_4	1.39	4.54	14.03	0.099	0.323
BeF_4	1.83	4.53	44.99	0.041	0.101
BO_3	2.17	4.25	24.47	0.089	0.173
BO_4	1.84	5.09	19.16	0.096	0.266
NaO_4	2.3	7.22	21.21	0.108	0.341
NaF_6	1.24	7.16	24.66	0.050	0.291
MgN_4	3.08	8.76	20.81	0.148	0.421
MgO_4	2.29	6.07	23.82	0.096	0.255
MgO_6	1.91	10.89	18.92	0.101	0.575
MgF_6	2.00	9.06	33.58	0.060	0.270
AlN_4	2.77	6.94	21.30	0.130	0.326
AlN_6	2.34	19.57	16.85	0.139	1.161
AlO_4	2.72	8.10	31.71	0.086	0.255
AlO_5	2.45	15.35	23.91	0.102	0.642
AlO_6	2.27	13.44	22.06	0.103	0.609
AlF_6	2.69	11.21	47.17	0.057	0.238
SiN_4	3.13	7.71	24.86	0.126	0.310
SiN_6	2.56	12.45	17.15	0.149	0.726
SiO_4	3.21	6.61	49.33	0.065	0.134
SiO_6	2.66	17.15	23.61	0.112	0.726
HfO_6	5.17	31.84	32.22	0.120	0.737
HfO_7	4.61	40.24	34.48	0.134	1.167
HfO_8	4.49	53.40	32.36	0.139	1.650
HfN_8	4.63	52.39	24.99	0.185	2.096

Table 1. Electronic polarizabilities (α in Å^3), ionic oscillator strengths (η in Å^3), effective volumes (V in Å^3), electronic polarizabilities per volume (α/V), and ionic oscillator strengths per volume (η/V) of 26 coordination polyhedra.

concluded that our η values of MgO_4, MgO_6, AlO_4, AlO_5, AlO_6, SiO_4, and SiO_6 coordination polyhedra are reliable.

To test the applicability of our model, we evaluated permittivities of many ternary and quaternary oxides in $(MgO)_x(Al_2O_3)_y(SiO_2)_z$ system (see Table 2). DFPT results obtained by us and some experimentally or theoretically reported values are also listed in Table 2 for comparison. We can see that our model with optimized α and η is really helpful to evaluate materials permittivity. Moreover, our model may provide a way to obtain permittivity for very complex systems where DFPT approach is not feasible, e.g., enstatite $MgSiO_3$ (80 atoms/cell) listed in Table 2.

However, one must keep in mind the limitations of the model (see η values shown in Fig. 1). We conclude that our simplified model is not suitable for materials with low-frequency polar modes having large contributions (due to large η values) to the lattice permittivity. We return to this point later in this paper.

Our model can also be extended to evaluate permittivity of a hypothetical structure, for which only the types of coordination polyhedra are given. To achieve this, we define volume V_i for each type of coordination polyhedron i, and determine optimal V_i values in the same way as for α_i and η_i (as listed in Table 1). The addition of V_i of coordination polyhedron i can reproduce volume of a structure well (as shown in Fig. 2). Then the α/V (η/V) values of a structure can be obtained from:

$$\alpha/V = \sum_i n_i\alpha_i / \sum_i n_i V_i, \text{ and } \eta/V = \sum_i n_i\eta_i / \sum_i n_i V_i.$$

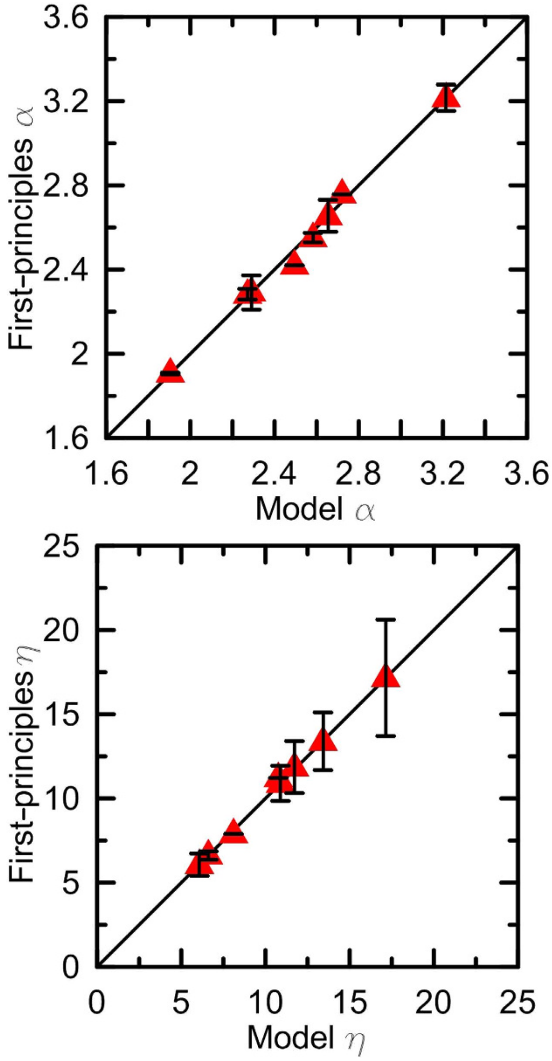

Figure 1. Characteristic parameters α and η. Comparison between characteristic parameters α (in Å^3) and η (in Å^3) of many MgO, Al_2O_3, and SiO_2 phases calculated from DFPT and those derived from optimal α_i and η_i values reported for coordination polyhedron *i*.

The corresponding α/V (η/V) values are comparable to those calculated from DFPT approach (see Fig. 3). In this way, permittivity of a hypothetical structure can be reasonably evaluated.

Application of the model. The α, η, and V values of each type of coordination polyhedra obtained from our model are helpful to design dielectric materials with expected permittivity. First, we extended our model to study some other oxides, nitrides, and fluorides (see Supplementary Table IIs). We obtained α, η, and V values for another 19 coordination polyhedra (see Table 1). With the α, η, and V values of 26 coordination polyhedra listed in Table 1, we illustrated how to rationally design ferroelectric, and high/low permittivity materials.

We have calculated ε_L of 95 compounds using η values of these 26 coordination polyhedra. Some of these compounds are listed in Table 2. The complete list of compounds can be found as Supplementary Tables Is and IIs. We compare ε_L values of these 95 compounds with those calculated from DFPT approach (see Fig. 4). The agreement between the two data sets is good. However, there are two deviating structures, *P4$_2$/nmc* HfO_2 and *Pbnm* $MgSiO_3$, for which the actual ε_L is much higher than that from our model. We found that the "unusual" enhancement of ε_L is related to large η values. This may originate from low-frequency polar phonon modes, which means that these two structures can be close to a ferroelectric instability.

In fact, the *P4$_2$/nmc* HfO_2 is a well-known ferroelectric material. Another structure, *Pbnm* $MgSiO_3$, possesses a perovskite structure adopted by many ferroelectric materials. We calculated the contributions to ε_L from each polar phonon mode of *Pbnm* $MgSiO_3$ (as listed Table 3). The *Pbnm* $MgSiO_3$ indeed

Compound	SG	ε_∞ model	ε_∞ DFPT	ε_∞ reported	ε_0 model	ε_0 DFPT	ε_0 reported
$MgAl_2O_4$ (Spinel)	$Fd\bar{3}m$	3.18	3.06	2.89[34]	9.27	8.51	8.40[35],8.75[36]
$MgAl_2O_4$ ($CaFe_2O_4$-type)	*Pbnm*	3.46	3.31		11.36	15.13	
$MgAl_2O_4$ ($CaTi_2O_4$-type)	*Cmcm*	3.36	3.30		11.07	14.46	
$MgSiO_3$ (Enstatite)	*Pbca*	3.11	–		7.35	–	8.23[37]
$MgSiO_3$ (Clinoenstatite)	$P2_1/c$	3.09	2.82		7.30	9.25	
$MgSiO_3$ (Protoenstatite)	*Pnab*	2.88	2.78		6.84	7.10	6.70[38]
$MgSiO_3$ (Clinoenstatite)	*C2/c*	2.88	2.78		6.83	7.31	
$MgSiO_3$ (Corundum)	$R\bar{3}$	3.20	3.15		11.00	10.07	
$MgSiO_3$ (Perovskite)	*Pbnm*	3.52	3.38		11.94	16.80	
Mg_2SiO_4 (Forsterite)	*Pbnm*	2.96	2.84	2.78[39]	7.76	7.52	6.80[40],7.30[41]
Mg_2SiO_4 (Wadsleyite)	*Imma*	3.21	3.01		8.39	8.45	
Mg_2SiO_4 (Ringwoodite)	$Fd\bar{3}m$	3.33	3.03		8.64	8.14	
Al_2SiO_5 (Andalusite)	*Pmnn*	2.78	2.83	2.78[42]	7.51	7.79	8.28[37],8.0[43]
Al_2SiO_5(Sillimanite)	*Pmcn*	2.97	2.88	2.85[42]	7.16	7.47	9.29[37],6.2[44]
Al_2SiO_5 (Kyanite)	$P\bar{1}$	3.24	3.09	3.14[42]	8.78	8.78	
$Mg_2Al_4Si_5O_{18}$(Cordierite)	*Cccm*	2.42	2.39		5.34	4.97	5.0[45],6.14[46]

Table 2. Space group (SG), and permittivities (electronic —ε_∞, and static—ε_0) of some ternary and quaternary oxides in the $(MgO)_x(Al_2O_3)_y(SiO_2)_z$ system.

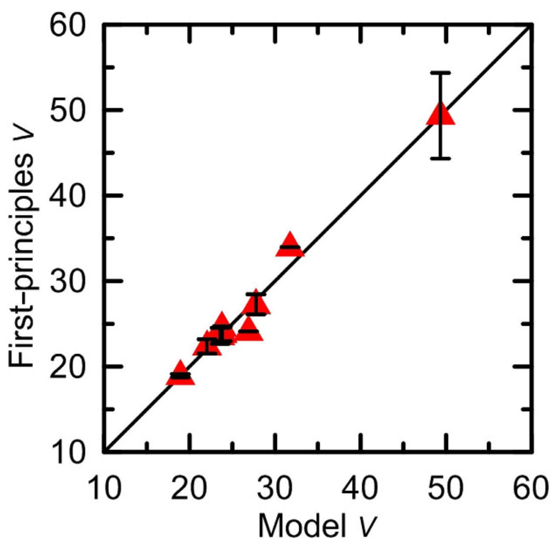

Figure 2. Volume *V*. Comparison between volume V (in Å^3) of many MgO, Al_2O_3, and SiO_2 compounds calculated from DFPT and those derived from optimal V_i values reported for coordination polyhedron i.

possesses a low-frequency polar phonon mode (at 175 cm^{-1}) contributing to ε_L much more than other phonon modes. In other words, our model underestimates permittivities of ferroelectrics and crystals with softened polar modes. This can actually be used for rapid screening of potential ferroelectric materials.

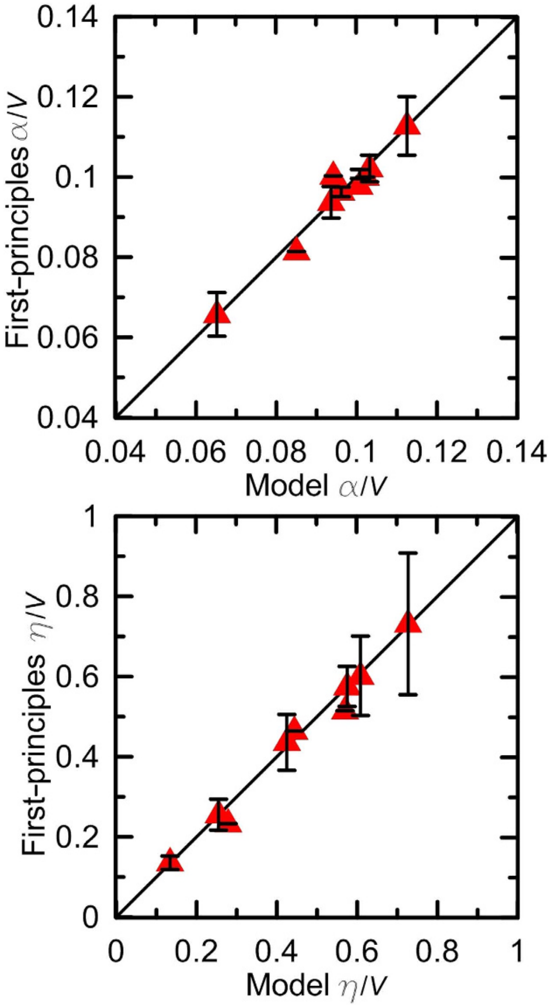

Figure 3. Parameters α/V and η/V. Comparison between parameters (α/V and η/V) of many MgO, Al_2O_3, and SiO_2 phases calculated from DFPT and those estimated by using α_i, η_i, and V_i values of coordination polyhedron i.

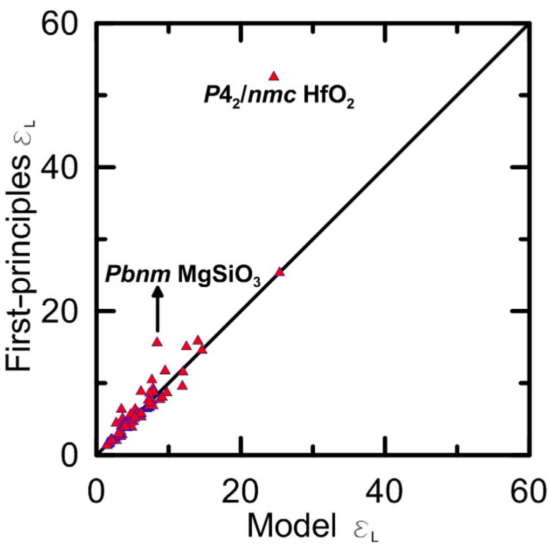

Figure 4. Lattice permittivity ε_L. Comparison between lattice permittivity ε_L of 95 compounds obtained by using the present simplified semi-empirical model and those calculated from DFPT.

Mode	$\omega[\mathrm{cm}^{-1}]$	$\Delta\omega$	Mode	$\omega[\mathrm{cm}^{-1}]$	$\Delta\omega$	Mode	$\omega[\mathrm{cm}^{-1}]$	$\Delta\omega$
B_{2u}	175	6.14	B_{2u}	430	1.83	B_{3u}	662	0.11
B_{3u}	239	0.61	B_{1u}	449	0.14	B_{1u}	688	~0
B_{1u}	253	0.24	B_{2u}	464	0.64	B_{2u}	690	0.02
B_{2u}	293	0.83	B_{3u}	474	2.02	B_{2u}	715	0.20
B_{1u}	307	1.80	B_{1u}	486	1.80	B_{3u}	737	0.22
B_{3u}	332	1.04	B_{3u}	514	0.07	B_{3u}	749	~0
B_{3u}	367	0.23	B_{1u}	541	~0	B_{1u}	760	0.16
B_{3u}	405	0.63	B_{1u}	582	0.37			
B_{1u}	416	0.30	B_{2u}	586	0.23			

Table 3. Frequencies of polar phonon modes ($\omega[\mathrm{cm}^{-1}]$) and their contributions to the permittivity ($\Delta\omega$) computed for *Pbnm* $MgSiO_3$[46].

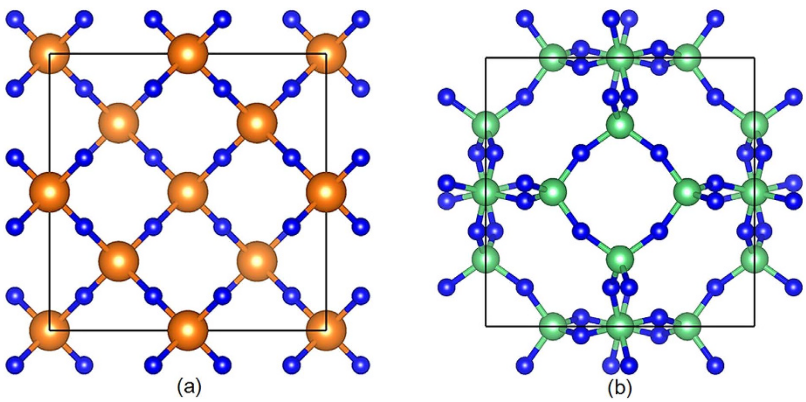

Figure 5. Crystal structures of MgF_2 and BeF_2. (**a**) $Fd\bar{3}m$ MgF_2 constructed from MgF_4 coordination polyhedra; (**b**) $I\bar{4}3m$ BeF_2 constructed from BeF_4 coordination polyhedra. Blue spheres denote F atoms, brown spheres denote Mg atoms, and green spheres denote Be atoms.

Our model is also helpful in the design of materials with high/low permittivity. Our results show, quite intuitively, that coordination polyhedra with high α (η), and low V are favorable for high dielectric permittivity.

At a glance at Table I, we can find that HfO_8 has much higher α/V and η/V values than others among the 26 coordination polyhedra. Indeed, Hf oxides are excellent high-permittivity oxides (ref. 20). On the other hand, SiO_4 tetrahedron possesses the lowest α/V and η/V values among O-based coordination polyhedra. Indeed, SiO_2 (quartz and silica glass) with SiO_4 tetrahedra is a well-known low-permittivity material in micro-electronics industry.

Noticeably, α/V and η/V values of N-based coordination polyhedra are higher than those of O-based coordination polyhedra. For instance, AlN_6 coordination polyhedron has much higher α/V and η/V values than AlO_6. We may expect high-permittivity in nitrides, e.g., Hf_3N_4 with HfN_8 coordination polyhedron. As listed in Table 1, α/V and η/Vvalues of HfN_8 coordination polyhedron are higher than those of the HfO_8 polyhedron. Therefore, $I\bar{4}3d$ Hf_3N_4 with HfN_8 coordination polyhedron has higher permittivities than most of hafnium oxides (see Supplementary Table IIs).

For the design of low-permittivity materials, we can immediately expect that permittivity of an oxide can be decreased by replacing O with F (see Table 1). Experimentally, SiF_4 material with SiF_4 tetrahedra has much lower permittivity than quartz[26,27]. In a similar way, we can expect that α/V and η/V values of MgF_4 coordination polyhedron may be much lower than those of MgO_4 polyhedron. Therefore, we try to design low-permittivity MgF_2 material with MgF_4 coordination polyhedron. We constructed a new $Fd\bar{3}m$ MgF_2 phase (Fig. 5(a)) with very low permittivity using $Fd\bar{3}m$ SiO_2 structure (cristobalite) with SiO_4 tetrahedra (detailed structural information can be found as Supplementary Table IIIs). The static permittivity ε_0 of $Fd\bar{3}m$ MgF_2 (2.5) is much lower than that of quartz (3.9[27]) and comparable to most low-permittivity polymers. The dynamical and mechanical stability of $Fd\bar{3}m$ MgF_2 was verified by phonon and elastic constants calculations (see Supplementary Fig. 1s and Table IVs). The enthalpy of $Fd\bar{3}m$ MgF_2 phase is only 0.1 eV/atom higher than that of the most stable MgF_2 structure ($P4_2/mnm$

phase). Moreover, this inorganic material may have a better mechanical strength than polymers (see Supplementary Table IVs). This suggests that $Fd\bar{3}m$ MgF_2 may be synthesized and tested as a potential low-permittivity material.

From the Materials Project, we also found a near-ground-state BeF_2 structure ($I\bar{4}3m$) with BeF_4 coordination polyhedra, as shown in Fig. 5(b). The static permittivity ε_0 of $I\bar{4}3m$ BeF_2 is 2.5, indicating that BeF_2 is also a good low-permittivity material. We suggest that compounds constructed from LiF_4, BF_4, NaF_4, and AlF_4 coordination polyhedra may also have low permittivities, e.g., ε_0 of $P3_121$ $LiBF_4$ with LiF_4 and BF_4 coordination polyhedra can be as low as 3.6.

We have to mention that coordination number is an important factor to design high/low-permittivity materials. There is a trend[21,23]: low coordination number, low permittivity. Our present study agrees with this trend well; coordination polyhedra with low coordination number have low α/V and η/V values. For example, our study shows that the $Pn\bar{3}m$ SiC_2N_4 structure, with 1/3 SiN_4 and 2/3 CN_2 coordination polyhedra, has much lower permittivity (4.6) than $P6_3/m$ Si_3N_4 (8.3) containing SiN_4 coordination polyhedra.

To summarize, we have presented a method for designing new inorganic dielectrics with expected permittivity is discussed. Coordination polyhedron is adopted as the functional structural block (FSB) of permittivity. Three parameters (electronic polarizability α, ionic oscillator strength η, and volume V) are chosen to characterize each coordination polyhedron. We show applications of this model evaluate materials permittivity. Results derived from this model agree well with those from density-functional perturbation theory. Moreover, α, η, and V values assigned to coordination polyhedra may be helpful to make intuitive choices of materials to focus on. Successful applications include ferroelectric, high- and low-permittivity materials.

Methods

Before calculating the properties, we perform full structure relaxation using density functional theory (DFT[2,3]) as implemented in the Vienna *ab intio* Simulation Package (VASP[28]) with the PBEsol-GGA[29,30] exchange-correlation functional. The all-electron projector-augmented wave (PAW) method[31] is used, with a plane-wave energy cutoff of 900 eV and k-point meshes with reciprocal-space resolution of $2\pi \times 0.04\text{Å}^{-1}$. These settings enable excellent convergence for the energy differences, stress tensors, and structural parameters. With fully relaxed structures, dielectric[25] and mechanical[32] properties (e.g. the elastic constants) were computed. Permittivities and phonon dispersion curves are calculated using density functional perturbation theory (DFPT[25]). Phonon dispersion curves were obtained by PHONOPY[33].

References

1. Jain, A. *et al.* Commentary: The materials project: A materials genome approach to accelerating materials innovation. *APL Materials* **1,** 011002 (2013).
2. Hohenberg, P. & Kohn, W. Inhomogeneous electron gas. *Phys. Rev*. **136,** B864–B871 (1964).
3. Kohn,W. & Sham, L. J. Self-consistent equations including exchange and correlation effects. *Phys. Rev*. **140,** A1133–A1138 (1965).
4. Ma, R. *et al.* Rationally designed polyimides for high-energy density capacitor applications. *ACS Appl. Mat. Interfaces* **6,** 10445–10451 (2014).
5. Sharma, V. *et al.* Rational design of all organic polymer dielectrics. *Nature Commun*. **5,** 4845 (2014).
6. Duan, D. *et al.* Pressure-induced metallization of dense $(H_2S)_2H_2$ with high-T_c superconductivity. *Sci. Rep*. **4,** 6968 (2014).
7. Yu, L. & Zunger, A. Identification of potential photovoltaic absorbers based on first-principles spectroscopic screening of materials. *Phys. Rev. Lett*. **108,** 068701 (2012).
8. Yang, K., Setyawan, W., Wang, S., Nardelli, M. B. & Curtarolo, S. A search model for topological insulators with high-throughput robustness descriptors. *Nature Mater*. **11,** 614–619 (2012).
9. Lin, L.-C. *et al.* In silico screening of carbon-capture materials. *Nature Mater*. **11,** 633–641 (2012).
10. Greeley, J., Jaramillo, T. F., Bonde, J., Chorkendorff, I. & Nørskov, J. K. Computational high-throughput screening of electrocatalytic materials for hydrogen evolution. *Nature Mater*. **5,** 909–913 (2006).
11. Wang, S., Wang, Z., Setyawan, W., Mingo, N. & Curtarolo, S. Assessing the thermoelectric properties of sintered compounds via high-throughput *Ab-Initio* calculations. *Phys. Rev. X* **1,** 021012 (2011).
12. Armiento, R., Kozinsky, B., Fornari, M. & Ceder, G. Screening for high-performance piezoelectrics using high-throughput density functional theory. *Phys. Rev. B* **84,** 014103 (2011).
13. Lu, J., Fang, Z. Z., Choi, Y. J. & Sohn, H. Y. Potential of binary lithium magnesium nitride for hydrogen storage applications. *J. Phys. Chem. C* **111,** 12129–12134 (2007).
14. Jain, A. *et al.* A computational investigation of $Li_9M_3(P_2O_7)_3(PO_4)_2$(M = V, Mo) as cathodes for Li ion batteries. *J. Electr. Soc*. **159,** A622–A633 (2012).
15. Oganov, A. R. *Modern methods of crystal structure prediction* (John Wiley & Sons, 2011).
16. Oganov, A. R. & Glass, C. W. Crystal structure prediction using *ab initio* evolutionary techniques: Principles and applications. *J. Chem. Phys.* **124,** 244704 (2006).
17. Glass, C. W., Oganov, A. R. & Hansen, N. Uspex-evolutionary crystal structure prediction. *Comput. Phys. Commun.* **175,** 713–720 (2006).
18. Lyakhov, A. O. & Oganov, A. R. Evolutionary search for superhard materials: Methodology and applications to forms of carbon and TiO_2. *Phys. Rev. B* **84,** 092103 (2011).
19. Zhu, Q., Oganov, A. R., Salvadó, M. A., Pertierra, P. & Lyakhov, A. O. Denser than diamond: *Ab initio* search for superdense carbon allotropes. *Phys. Rev. B* **83,** 193410 (2011).
20. Zeng, Q. *et al.* Evolutionary search for new high-*k* dielectric materials: methodology and applications to hafnia-based oxides. *Acta Cryst.* **C70,** 76–84 (2014).
21. Xie, C., Zeng, Q., Oganov, A. R. & Dong, D. Discovering low-permittivity materials: Evolutionary search for $MgAl_2O_4$ polymorphs. *Appl. Phys. Lett.* **105,** 022907 (2014).

22. Rignanese, G.-M., Detraux, F., Gonze, X., Bongiorno, A. & Pasquarello, A. Dielectric constants of Zr silicates: A first-principles study. *Phys. Rev. Lett.* **89,** 117601 (2002).
23. Xie, C. *et al.* First-principles calculations of the dielectric and vibrational properties of ferroelectric and paraelectric $BaAl_2O_4$. *Phys. Lett. A* **378,** 1867–1870 (2014).
24. Blythe, A. R. & Bloor, D. *Electrical properties of polymers* (Cambridge University Press, 2005).
25. Baroni, S., de Gironcoli, S., Dal Corso, A. & Giannozzi, P. Phonons and related crystal properties from density-functional perturbation theory. *Rev. Mod. Phys.* **73,** 515–562 (2001).
26. Rado, W. G. The nonlinear third order dielectric susceptibility coefficients of gases and optical third harmonic generation. *Appl. Phys. Lett.* **11,** 123–125 (1967).
27. Robertson, J. High dielectric constant gate oxides for metal oxide Si transistors. *Rep. Prog. Phys.* **69,** 327 (2006).
28. Kresse, G. & Furthmüller, J. Efficient iterative schemes for *ab initio* total-energy calculations using a plane-wave basis set. *Phys. Rev. B* **54,** 11169–11186 (1996).
29. Perdew, J. P. *et al.* Restoring the density-gradient expansion for exchange in solids and surfaces. *Phys. Rev. Lett.* **100,** 136406 (2008).
30. Perdew, J. P., Burke, K. & Ernzerhof, M. Generalized gradient approximation made simple. *Phys. Rev. Lett.* **77,** 3865–3868 (1996).
31. Blöchl, P. E. Projector augmented-wave method. *Phys. Rev. B* **50,** 17953–17979 (1994).
32. Cowley, R. A. Acoustic phonon instabilities and structural phase transitions. *Phys. Rev. B* **13,** 4877–4885 (1976).
33. Togo, A., Oba, F. & Tanaka, I. First-principles calculations of the ferroelastic transition between rutile-type and $CaCl_2$-type SiO_2 at high pressures. *Phys. Rev. B* **78,** 134106 (2008).
34. Boguslavska, N. N., Venger, E. F., Vernidub, N. M., Pasechnik, Y. A. & Shportko, K. V. Reststrahlen spectroscopy of $MgAl_2O_4$ spinel. Semicond. *Phys. Quantum Electron. Optoelectron.* **5,** 95–100 (2002).
35. Wang, C. C. & Zanzucchi, P. J. Dielectric and optical properties of stoichiometric magnesium aluminate spinel single crystals. *J. Electrochem. Soc.* **118,** 586–591 (1971).
36. Surendran, K. P., Bijumon, P. V., Mohanan, P. & Sebastian, M. T. $(1-x)MgAl_2O_{4-x}TiO_2$ dielectrics for microwave and millimeter wave applications. *Appl. Phys. A* **81,** 823–826 (2005).
37. Rosenholtz, J. L. & Smith, D. T. *The dielectric constant of mineral powders* (Rensselaer Polytechnic Institute, 1936).
38. Song, M. E. *et al.* Synthesis and microwave dielectric properties of $MgSiO_3$ ceramics. *J. Am. Ceram. Soc.* **91,** 2747–2750 (2008).
39. De La Pierre, M. *et al.* Performance of six functionals (LDA, PBE, PBESOL, B3LYP, PBE0, and WCLLYP) in the simulation of vibrational and dielectric properties of crystalline compounds. the case of forsterite $MgSi_2O_4$. *J. Comput. Chem.* **32,** 1775–1784 (2011).
40. Ohsato, H., Tsunooka, T., Sugiyama, T., Kakimoto, K.-I. & Ogawa, H. Forsterite ceramics for millimeterwave dielectrics. *J. Electroceram.* **17,** 445–450 (2006).
41. Shannon, R. D. Dielectric polarizabilities of ions in oxides and fluorides. *J. Appl. Phys.* **73,** 348–366 (1993).
42. Aryal, S., Rulis, P. & Ching, W. Y. Density functional calculations of the electronic structure and optical properties of aluminosilicate polymorphs (Al_2SiO_5). *Am. Miner.* **93,** 114–123 (2008).
43. Eru, I., Peskovatskiy, S. & Chernets, A. Trivalent-iron-doped andalusite as crystal for microwave waves. *IEEE J. Quantum Electron.* **4,** 723–727 (1968).
44. Mugeraya, S. & Prabhakar, B. R. Measurement of resistivity and dielectric constant of beach-sand minerals. *J. Electrostat.* **18,** 109–112 (1986).
45. Sei, T., Eto, K. & Tsuchiya, T. The role of boron in low-temperature synthesis of indialite (α-$Mg_2Al_4Si_5O_{18}$) by sol–gel process. *J. Mater. Sci.* **32,** 3013–3019 (1997).
46. Ohsato, H. *et al.* Sintering conditions of cordierite for microwave/millimeterwave dielectrics. *IEEE Trans. Ultrason. Ferroelectr. Freq. Control.* **55,** 1081–1085 (2008).

Acknowledgements
This work was supported by the Foreign Talents Introduction and Academic Exchange Program of China (No. B08040), the National Science Foundation (EAR-1114313, DMR-1231586), DARPA (Grant No. W31P4Q1210008), and the Government of Russian Federation (grant 14.A21.31.0003). The authors also acknowledge the High Performance Computing Center of NWPU for the allocation of computing time on their machines.

Author Contributions
C.-W.X. and A.R.O. designed the project and performed the calculations. C.-W.X., A.R.O. and D.D. analyzed the data, and wrote the paper. N.L. got the structural information of the structures studied in this paper. D.L. and T.T.D. helped to plot the figures.

Additional Information
Supplementary information accompanies this paper at http://www.nature.com/srep

Competing financial interests: The authors declare no competing financial interests.

How to cite this article: Xie, C. *et al.* Rational design of inorganic dielectric materials with expected permittivity. *Sci. Rep.* **5**, 16769; doi: 10.1038/srep16769 (2015).